

## Friction in a thin commensurate contact

Oleg M. Braun

*Laboratoire de Physique, URA-CNRS 1325, ENS de Lyon, 69364 Lyon Cédex 07, France  
and Institute of Physics, Ukrainian Academy of Sciences, Kiev UA-252022, Ukraine*

Thierry Dauxois and Michel Peyrard

*Laboratoire de Physique, URA-CNRS 1325, ENS de Lyon, 69364 Lyon Cédex 07, France*

(Received 14 April 1997)

The dynamics of a thin layer of atoms between two rigid substrates is studied by molecular dynamics. Simulations exhibit different regimes. For a low relative velocity of the substrates a stick-slip regime concerning alternating atomic channels, which is reminiscent of intermittency in chaotic systems, is observed. At a high velocity the system reaches a sliding regime, for which the simulation results can be described by an effective intrinsic friction due to an energy exchange between the moving top substrate and the atomic film. [S0163-1829(97)06332-7]

### I. INTRODUCTION

The problem of friction between two substrates which are in moving contact, is a very important technological problem as well as a very interesting physical question.<sup>1-3</sup> It can be considered at several levels. The *macroscopic* level was studied since the 18th century, mostly empirically, for technological applications. More recently the *mesoscopic* level was studied in an attempt to derive the experimental laws observed earlier<sup>4</sup> using the idea that real contacts between the substrates take place at small regions which are linked by elastic interactions. This approach successfully explains a stick-slip effect. Finally, tribology currently approaches the *microscopic* level by the study of the contacts themselves. This approach expanded after the development of the atomic force microscopy, which allows the experimental study of friction in a very small contact, and because nanotechnology is now beginning to build devices that are so miniaturized that they begin to probe the microscopic properties of the materials.

Microscopic investigations can use different approaches. Besides the atomic force microscopy that brings experimental data, molecular dynamics (MD) with realistic potentials may be useful to provide very detailed information on atomic motions, the distribution of energy among different modes, etc. But the simulations can become extremely heavy, particularly when three-dimensional calculations are performed. An alternate route is to use microscopic modeling which does not attempt to include all degrees of freedom. A first model can consider one atomic layer sitting over a two-dimensional periodic potential that describes the lower substrate, and driven by an external force corresponding to the stress inducing the motion of the top substrate over the lower one. This approach was considered by Persson<sup>1</sup> and in our previous paper.<sup>5</sup> It was then extended to a bilayer of atoms adsorbed on the silver-coated surface of the vibrating quartz crystal of a microbalance.<sup>6</sup> In this case the layer is driven on one side only and the sliding is due to its inertia. The present work intends to analyze the situation of boundary layer friction in which the intermediate layer is subjected to stress

coming from both sides, while staying at a simpler level than full molecular dynamics. We consider three atomic layers, henceforth called the ‘‘lubricant film,’’ situated between two solid substrates. The value of three was chosen because it allows the top and bottom lubricant layers to stick to the substrate while leaving mobile atoms in between.

The problem of friction has two different sides. Studies of *static friction* intend to determine the minimum driving that will cause the top substrate to slide. We shall here consider *dynamical friction* for which the main question that one may ask when considering the system at the macroscopic scale is the relation between the sliding velocity  $v_s$  and the driving. They are related by the mobility coefficient  $B$  defined as

$$v_s = Bf, \quad (1)$$

where  $f$  is the force per atom applied to the top substrate. The mobility is determined by an exchange between the kinetic energy of the moving substrate and the phonons and electronic degrees of freedom in the system. To describe it properly, two essential points should be taken into account. *First*, the classical MD approach, even with a realistic interaction potential, only considers the phonon degrees of freedom. But for metal or semiconductor substrates, the electronic degrees of freedom are important as well, because the kinetic energy of the substrates may be transformed not only into phonons, but also into excitation of electron-hole pairs. A similar problem emerged in studies of surface diffusion,<sup>7</sup> where the classical MD technique gives too high diffusion coefficients. One solution to the problem is to add an external friction  $\eta$  to the equations of motion, i.e., to study Langevin equations of motion instead Newtonian ones. The value of  $\eta$  has to be chosen to describe phenomenologically the energy loss into electron-hole formation. *Second*, for a correct description of the phonon mechanism of energy exchange, the phonon density of states must be modeled correctly. But the density of states depends drastically on the dimensionality of the system (e.g., see Ref. 8); the one-, two-, and three-dimensional systems have qualitatively different spectra. Therefore, a realistic model *must* be three di-

dimensional which makes MD simulations with realistic interatomic potentials extremely time consuming. To understand the energy loss into phonons, notice that the force applied to the atoms within the sliding layer has an oscillatory component at frequency

$$\omega_s = 2\pi v_s / a_s, \quad (2)$$

where  $a_s$  is the lattice constant, due to alternating bond breaking and bond forming as the substrate moves. As discussed below this component can excite vibrations of the lubricant film.

Recalling the Brownian motion of a particle of mass  $m$  in a viscous medium, where the velocity follows the law  $v = B_{ff}$  with  $B_f = (m\eta)^{-1}$ , we shall write the mobility  $B$  under the form

$$B = (m_{\text{eff}}\eta_{\text{eff}})^{-1}, \quad (3)$$

where the parameters  $m_{\text{eff}}$  and  $\eta_{\text{eff}}$  have to be found theoretically. Notice that, according to the definition (1) of  $B$  with the force  $f$  per atom of the substrate, the extensive quantities entering in the expressions (the masses) are defined for one unit cell of the substrate. The effective moving mass  $m_{\text{eff}}$  in Eq. (3) takes into account the fact that a part of the film may stay attached to the top substrate and therefore moves together with it. Therefore it can be written

$$m_{\text{eff}} = m_s + m_a \theta_a, \quad (4)$$

where  $m_s$  and  $m_a$  are the masses of substrate and film atoms, respectively, and  $\theta_a$  describes the number of film layers attached to the top substrate. The effective friction may be written in the form

$$\eta_{\text{eff}} = \eta + \eta_a, \quad (5)$$

i.e., as the sum of the external friction  $\eta$  artificially introduced into the model to describe the energy loss into electronic degrees of freedom, and the ‘‘intrinsic’’ friction  $\eta_a$  which is due to the energy flux from the moving top substrate into the phonon degrees of freedom of the film. One may expect that  $\eta_a$  will depend first of all on the frequency  $\omega_s$  associated with the motion of the substrate in relation with the phonon spectrum of the film. The main result of the present work is that at least in the sliding regime, i.e., at high enough velocity of the top substrate, this approach does explain the dynamical friction.

The paper is organized as follows. In Sec. II we describe the model and computer algorithm. In Sec. III the simulation results are presented. In Sec. IV these results are discussed along the lines defined by Eqs. (3)–(5) and the friction is evaluated by examining the phonon mechanism of energy loss. Finally, Sec. V concludes the paper.

## II. THE MODEL

We study a three-dimensional system consisting of an atomic film between two solid substrates called top and bottom substrates. Each substrate has  $N_s$  atoms of mass  $m_s$  organized into a square  $M_s \times M_s$  lattice with the lattice constant  $a_s$ . The thin atomic film situated between the substrates consists of  $N_a$  atoms of mass  $m_a$ . In the  $x$  and  $y$  directions we use periodic boundary conditions. The atoms of the bot-

tom substrate are immobile, while the top substrate may move as a whole, i.e., the relative arrangement of its atoms is fixed. The atoms of the film, as well as the top substrate, are allowed to move along the three directions of space  $x$ ,  $y$ , and  $z$ . All the atoms interact via the 6-12 Lennard-Jones potential,

$$V^{(x)}(r) = V_x [(r_x/r)^{12} - 2(r_x/r)^6], \quad (6)$$

so that the corresponding characteristic frequency of a particle of mass  $m$  at the bottom of the interaction potential is  $\omega_x = 6(2V_x/mr_x^2)^{1/2}$ . The interaction parameters  $V_x$  and  $r_x$  are different for the interaction within the film, ‘‘ $x=a$ ,’’ and the interaction of the film atoms with the top and bottom substrates, ‘‘ $x=0$ .’’ This allows us to simulate a lubricant between two solids or the effect of surface coating by a material that differs from the bulk. The two substrates are pressed together by a force  $f_{\text{load}}$  along the  $-z$  direction, applied to each atom of the top substrate.

To each atom of the top substrate we apply a d.c. force  $f$  along the  $x$  axis and then solve the Langevin equations for this atomic system in the presence of an external viscous friction with the coefficient  $\eta$ , which models the electron-hole energy exchange mechanism as discussed in Sec. I.

In this work, as we do not attempt to describe a specific material, we work with dimensionless quantities. The numerical values of the model parameters have however been chosen in such a way that, if energy were measured in eV and distances in Å, we would get realistic values for a solid. As we chose a mass  $m_a = 1$  for the particles of the film, this would set a time unit of the order of  $10^{-13}$  s for atoms weighting ten atomic mass units. We took  $a_s = 3$  for the substrate lattice constant, and  $V_0 = 3$  and  $r_0 = 3$  for the interaction of the atoms of the film with the substrates. With these parameters, a typical frequency for the system is  $\omega_0 = 6(2V_0/mr_0^2)^{1/2} = 4.90$ , and the corresponding characteristic period is equal to  $\tau_0 = 2\pi/\omega_0 = 1.28$ .

For the parameters of the interatomic interaction within the film, we took  $V_a = 1$ . Because  $V_a \ll V_0$ , some atoms of the film tend to stay attached to the top and bottom substrates, covering them with full monolayers, while the other film atoms fill the space between these monolayers. For the equilibrium distance  $r_a$  corresponding to the minimum of  $V^{(a)}(r)$  we study only the *commensurate* case with  $r_a = a_s = 3$ .

The simulations have been performed according to the following procedure. First, we apply the constant d.c. load force  $f_{\text{load}} = -0.1$  in the  $z$  direction to every atom of the top substrate to model the pressure applied to the contact. Then, starting with an appropriate initial configuration chosen as the closely packed structure, we allow the system to relax at zero temperature with the external friction  $\eta = \omega_0$  until it reaches the ground state. The relaxation continues until the inequality  $\sum_i N_a (\Delta r_i^2 + \Delta v_i^2) < 10^{-8}$  is fulfilled, where  $\Delta r_i$  and  $\Delta v_i$  are the change in the coordinate and velocity of the  $i$ th atom, respectively, during the time  $3\tau_0$ . Then the external friction in Langevin equations is set to  $\eta$  (typically  $\eta = 0.1\omega_0$ , see below Sec. III), and the temperature is increased by small steps (usually 100 steps) during the time

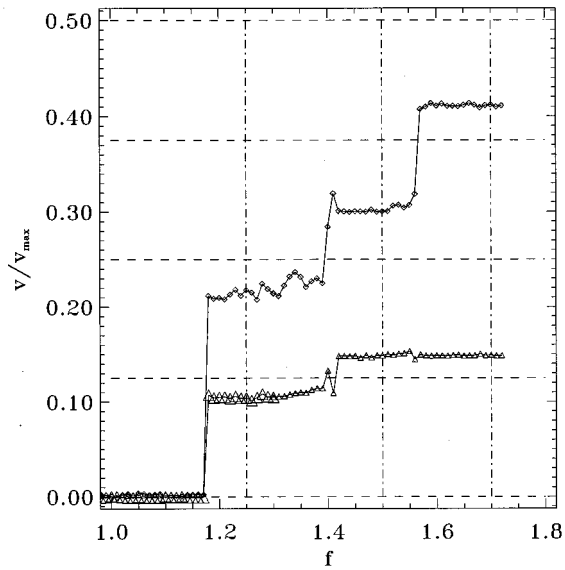


FIG. 1. The normalized velocities  $v/v_{\max}$  versus  $f$  for the three-layer commensurate film ( $N_a=300$ ,  $N_s=100$ ,  $m_s=1$ , and  $\eta=0.1\omega_0=0.489$ ). Diamonds correspond to the velocity of the top substrate, while triangles correspond to the velocity averaged over all 300 atoms of the film. The vertical dot-dashed lines indicate the values of the force studied in more detail and discussed in the text.

$t_1=100\tau_0$  until it reaches the value  $T=0.025$  which would correspond to room temperature for energies measured in eV.

After this period during which the system equilibrates at the temperature  $T$  we start the investigation of the friction by applying a shear force  $f$  to every top substrate atom along the  $x$  direction. The force is increased by small steps, usually  $\Delta f=0.01$ . Each increase of shear stress is accomplished progressively in  $t_2/\tau_0$  substeps (typically 100 substeps). When  $f$  has reached its new value, at the end of a sequence of increase, we wait during a time  $t_3$  in order to allow the system to reach a stationary state, and then we measure the atomic coordinates and velocities during the time  $t_4$  (usually  $t_3=t_4=100\tau_0$ ), saving them at each  $\Delta t=\tau_0$ .

### III. SIMULATION RESULTS

For the commensurate case studied in the present paper, we took  $r_a=a_s=3$ , so that  $\omega_a=2.83$ . The top and bottom substrates are made of  $N_s=100$  atoms ( $10\times 10$  square lattice). Between the substrates we set  $N_a=300$  atoms, i.e., the intermediate film consists of three layers. Because we took  $V_0\gg V_a$ , two of the layers are attached to the top and bottom substrates, and the interesting dynamics takes place in the third (middle) layer lying in between. The mass of an atom of the top substrate is  $m_s=1$ . The external friction is  $\eta=0.1\omega_0=0.489$ .

Figure 1 summarizes the simulation results. It shows the velocity of the top substrate  $v_s$  and the average film velocity  $v_a$  as the functions of the driving force  $f$ . Each data point is the average over 100 points recorded at time moments separated by  $\Delta t=\tau_0$ . The velocities are normalized with the value  $v_{\max}=f/(m_s\eta)$  which corresponds to the maximum velocity of the top substrate at a given driven force  $f$  if the

interaction between the top substrate and the film is absent. The simulations reveal a complex dynamical behavior. One can clearly see from Fig. 1 that the range of driving forces that we investigated splits into the following intervals corresponding to different regimes.

(i) At low forces,  $f\leq 1.17$ , the top substrate is immobile. The value  $f_s=1.17$  corresponds to the static frictional force. Recall that a single particle subjected to one-dimensional sinusoidal potential and driven by a force  $f$ , starts to move at forces  $f>\pi\epsilon_s/a_s$ , where  $\epsilon_s$  is the amplitude of the external potential. Thus, the barrier for the motion of one film's layer over another can be estimated as  $\epsilon_s\approx f_s a_s/\pi=1.12$ . On the other hand, the atom sitting over the square lattice in the minimum-energy position has the energy  $-4V_a$ , while in the saddle position its energy is about  $-2V_a$ , so that for the rigid motion of one layer over another the barrier is  $\approx 2V_a=2$ . As we find that the motion starts for a lower threshold, this indicates that it does not start for all atoms simultaneously, but emerges at some local fluctuations in the structure. This is to be expected for pinned incommensurate structures which contain a hierarchy of defects with various degrees of pinning<sup>9</sup> and it has been observed in numerical simulations of a single layer.<sup>2</sup> In the commensurate case that we investigate here, the origin of the local initiation of the sliding cannot be attributed to a hierarchy of depinning sites but it must lie in thermal fluctuations.

(ii) For the force within the interval  $1.17<f<1.40$  the velocity of the film averaged over all atoms is approximately equal to half the top substrate velocity. This regime corresponds to a ‘‘chaotic’’ regime showing some intermittency. The point  $f=1.25$  is studied in detail below.

(iii) For intermediate forces,  $1.40<f<1.57$ , the dynamics of the middle-layer differs for atoms situated in different channels, i.e., along different lines parallel to the driving direction  $x$ . The channels split approximately to even-odd ones, where even channels always move together with the top layer, while odd channels periodically move and stop with a period of about  $2\tau_0$ . A long term investigation of this intermediate regime for the force  $f=1.50$  showed that after a time of about  $10^3\tau_0$  the systems jumps to the sliding state described below. This indicates that the intermediate regime is not stable and it seems therefore unlikely that it can be observed experimentally, this is why we will not discuss it further.

(iv) For large forces,  $f>f_r=1.57$ , the top substrate starts to slide taking with it the upper layer of the film. In the middle layer one of the channels continues to move during some time, while others are generally fixed. From time to time they start to move, almost all simultaneously, for a short time interval and then stop again. The point  $f=1.70$  is discussed in more detail below.

All these regimes are separated by sharp (first-order) transitions, and if the force decreases, the system exhibits hysteresis. For instance, while the transition from locked to moving states occurs at  $f_s=1.17$  while forces increase, as shown in Fig. 1, the reverse transition to the locked state occurs at  $f_s=0.99$  when the force is reduced. The time dependences of velocities for three characteristic forces  $f=1.25$ ,  $f=1.50$ , and  $f=1.70$  taken to be within the intervals (ii), (iii), and (iv), respectively, are shown together in Fig. 2. These results show that, when one considers a lubri-

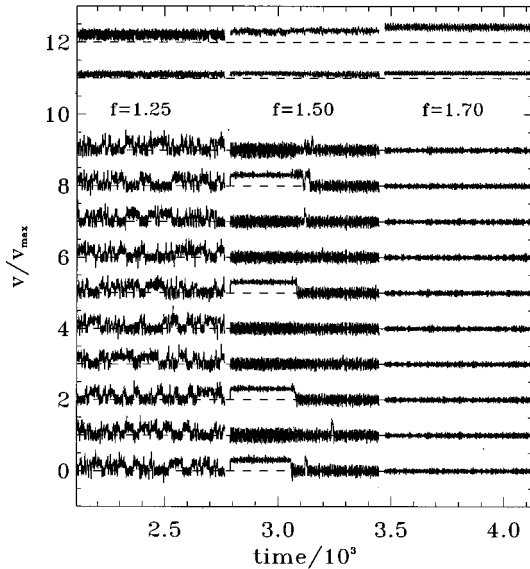


FIG. 2. Time dependences of the velocities for three characteristic forces  $f=1.25$  (left),  $f=1.50$  (middle), and  $f=1.70$  (right). The two upper curves present  $v_s$  (velocity of the top substrate) and  $v_a$  (velocity averaged over all 300 atoms), respectively. The other ten curves show the velocity of atoms in the middle layer only, each curve corresponding to one of the ten “channels,” i.e., it shows the velocity averaged over ten atoms in a given channel. Except for the lowest curve, all other curves are arbitrarily shifted upward for clarity.

cant film made of many interacting particles, the friction properties are much more complicated than in the case of a single particle between two substrates,<sup>3</sup> although the one-particle case was already very rich. One may wonder whether some generic properties can be extracted from these results or whether each case must be considered as specific. We show below that the analysis of representative cases may allow us to propose some general ideas that underlie the behavior of the system, and, in particular, that the simple description presented in Sec. I can provide useful results.

#### A. Case $f=1.25$

In this “chaotic” regime the lower layer of the film is immobile, the upper layer moves together with the top substrate, and the middle layer oscillates between two regimes in a state which suggests a phenomenon of intermittency. In the middle layer, the atoms belonging to a line along the  $x$  axis, that we call a channel, have highly correlated motions, as shown in Fig. 3. Figure 2 (left part) indicates that each channel chaotically jumps between an immobile and a running state, clinging to the top or bottom substrates for times much longer than  $\tau_0$ . The average velocity of the atoms of the film is equal to  $v_a/v_{\max}=0.104$ , and the average velocity of the middle-layer atoms only is  $v_{\text{middle}}/v_{\max}=0.102$ , both values being approximately two times smaller than the average velocity of the top substrate,  $v_s/v_{\max}=0.214$ . These data are consistent with a lower layer attached to the bottom substrate, a top layer moving together with the top substrate and a middle layer moving on average at the medium speed. As mentioned above this intermediate speed of the middle layer

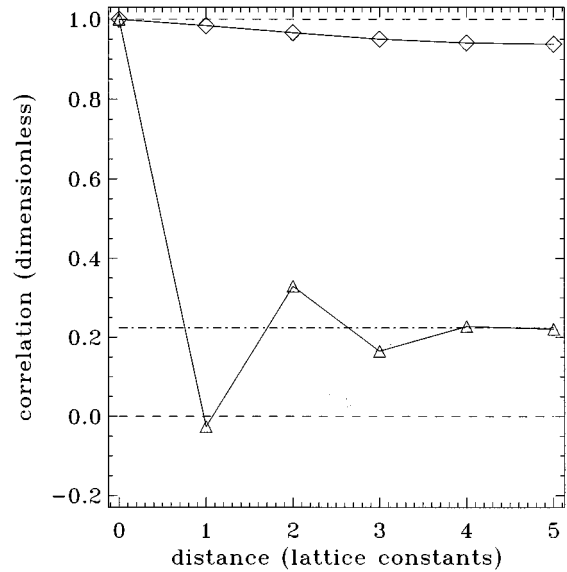


FIG. 3. The normalized correlation function of the velocities of the middle-layer atoms along the channels (diamonds) and between the channels (triangles, the long-distance level is shown by the dot-dashed line).

is in fact achieved by a stop-and-go mechanisms for the channels that make this layer. The typical  $v(t)$  dependencies for the middle-layer channels shown in Fig. 2 (left) clearly indicate an anticorrelation of the velocities of nearest-neighboring channels, while next-nearest-neighboring channels exhibit a small correlation. The calculated correlation function confirms this effect (see Fig. 3), and also shows that at large distances between the channels the interchannel correlation function tends to a nonzero limit due to long-range interaction through the top (rigid) substrate.

The interchannel correlations may be qualitatively explained in the following way. As the  $N_{\text{ch}}$  particles of a channel move together, let us describe a channel by a single mass  $m_{\text{ch}}$  driven by a force  $f_1=N_{\text{ch}}f$ . From previous studies on a single atomic layer mobile over a periodic potential,<sup>5</sup> we know that one can expect a running state for  $f_1>f_{c1}$ , where  $f_{c1}$  is some threshold force. Then the running state persists even when the driving is reduced, as long as  $f_1>f_{c2}$ , where  $f_{c2}$  is another threshold force for the back transition from the running state to the pinned state ( $f_{c2}<f_{c1}$ ). The behavior observed for  $f=1.25$  can be understood if  $f_1$  belongs to the domain  $f_{c2}<f_1<f_{c1}$ , i.e., we are below the running transition. Therefore, because  $f$  was progressively raised, for a single driven channel, we should be in the pinned state. This would be the case if all the channels were aligned on their equilibrium position as in Fig. 4(a). In this case a channel is only subjected to the external driving  $f_1$ . However this state is probably not stable if  $f_1$  is close to  $f_{c1}$ . Indeed, let us imagine that the straight line of “aligned channels” gets disturbed as in Fig. 4(b). Now a given channel is also subjected to additional forces exerted by its neighbors. The sum of the forces, projected on the  $x$  axis, may exceed  $f_{c1}$ . This will be the case for the channels which lag behind. They will start to move and tend to pass beyond their neighbors until the backward forces due to the interaction with the neighbors reduce the total projection below  $f_{c2}$ . Then the moving chan-

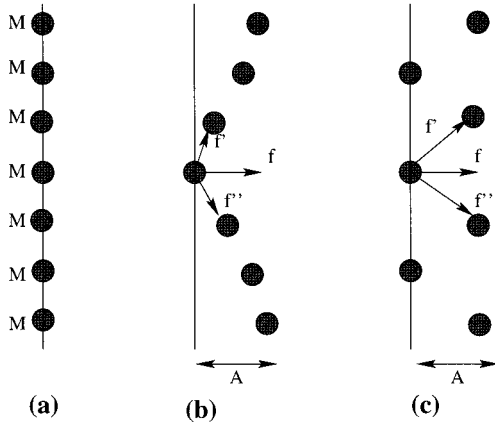


FIG. 4. Schematic figure of the forces acting on the moving channels. Each channel is represented by a single particle of mass  $M$ . (a) Particles in the channels are aligned as in the equilibrium state. The forces within the film cancel each other and the only force on a channel comes from the driving. (b) Some channels have moved with respect to others but adjacent channels have similar motions. In addition to the driving a channel is subjected to forces exerted by the neighboring channels. If the wavelength of the modulation of the motion is large, the additional forces are weak. (c) For a given amplitude of the modulation  $A$ , the additional forces due to neighboring channels are maximum if the modulation of the displacement of the channels has a wavelength of two lattice spacings.

nels will stop, but, as they have passed their neighbors, they pull the neighbors, which in turn start to move and the stop-and-go process will continue with other channels. As shown in Fig. 4(c), for a given amplitude of the modulation of the respective positions of the channels, the process creates the largest forces if two channels move in *anticorrelation*.

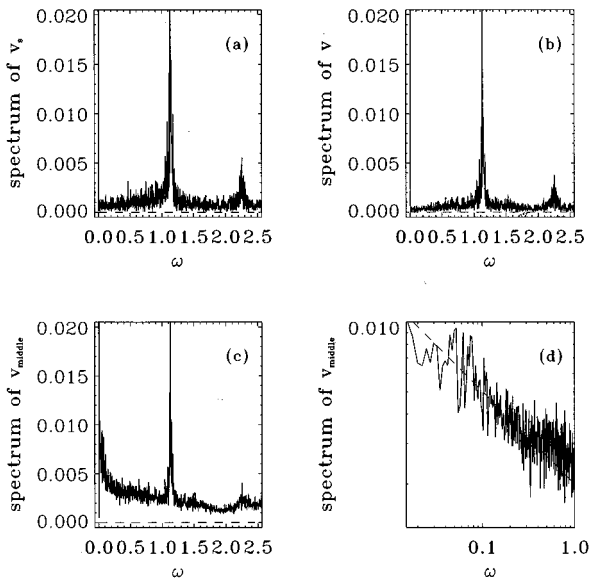


FIG. 5. Fourier transform of the velocities: (a) the top substrate velocity, (b) the velocity averaged over all 300 film's atoms, (c) the velocity averaged over 100 middle-layer atoms, (d) the same as (c) but in log-log scale, the dashed line corresponds to a  $0.02\omega^{-0.4}$  dependence.

The Fourier transform of the velocities presented in Fig. 5 shows a peak at  $\omega = 1.133$  which is close to the characteristic frequency  $2\pi v_s/a_s = 1.145$  corresponding to the frequency at which the mobile substrate excites the film through a sequence of bond breaking and bond forming. At low frequencies,  $\omega < 1$ , the spectrum of middle-layer atoms is continuous as typical for chaotic motion, and fits to a power law  $\tilde{v}(\omega) \propto \omega^{-0.4}$  which again is typical for a chaotic behavior with intermittency, where the power spectrum [defined as the Fourier transform of  $v^2(t)$ ] follows a power law with an exponent 0.8–1.4.<sup>10</sup>

### B. Case $f = 1.70$

For a large driving force the film splits into two parts. The top substrate, together with the upper film layer, slides over the bottom substrate with two film layers. The Fourier transform of the velocities shows a peak at  $\omega = 3.014$  which is close to the characteristic frequency  $2\pi v_s/a_s = 3.110$ , and moreover the spectrum shows higher harmonics multiple of this frequency, which indicates that the top substrate oscillations are anharmonic. The top substrate velocity,  $v_s/v_{\text{max}} = 0.427$ , is approximately three times larger than the average velocity of the atoms of the film,  $v_a/v_{\text{max}} = 0.141$ . This is consistent with a motion of only one third of the atoms of the film at a velocity close to that of the top substrate. A calculation of average velocity of only the upper-layer atoms gives  $v_{\text{up}}/v_{\text{max}} = 0.425$ , the value which is slightly lower than that of the top substrate.

### C. Variation of the external friction

To check the applicability of Eqs. (3)–(5), we made a series of runs for the 300-atomic commensurate film with different values of the external friction  $\eta$ , changing it from a low value  $\eta = 0.03\omega_0 = 0.15$  to a quite high value  $\eta = 0.20\omega_0 = 0.98$ . We calculated the dependences  $v_s(f)$  and then extracted the value of the intrinsic friction  $\eta_a$  with Eqs. (3)–(5) assuming  $\theta_a = 1$  in Eq. (4). The values of  $\eta_a$  for all the external frictions  $\eta$  are plotted together in Fig. 6 as a function of  $\omega_s = (2\pi/a_s)v_s$ . The fact that all points fit rather well on a single curve shows that the simple expressions (3)–(5) describe the essential features of the sliding regime and that it is meaningful to define an intrinsic friction  $\eta_a$  independent of  $\eta$ . Let us analyze the origin of this intrinsic friction by considering the different sources of energy dissipation in a simulation. As the atoms of the top substrate move as a whole, their contribution to the energy loss is  $m_s\eta v_s^2$ . Similarly, for the moving part of the film, a contribution  $m_a\eta v_s^2$  describes the energy loss due to the externally imposed friction that comes from the average velocity  $v_a \approx v_s$ . The only possible source for an extra dissipative term corresponding to the nonzero value of  $\eta_a$  must come from the *internal dynamics of the moving part of the film* which is not described by the average velocity  $v_a$ . This indicates that it comes from an oscillatory component of the motion of the film, which is characterized by the frequency  $\omega_s = (2\pi/a_s)v_s$ . When  $\omega_s$  lies within the phonon spectrum of the film,  $\Omega_{\text{min}} < \omega_s < \Omega_{\text{max}}$ , the sliding excites harmonic vibrations inside the film, and they are responsible for the

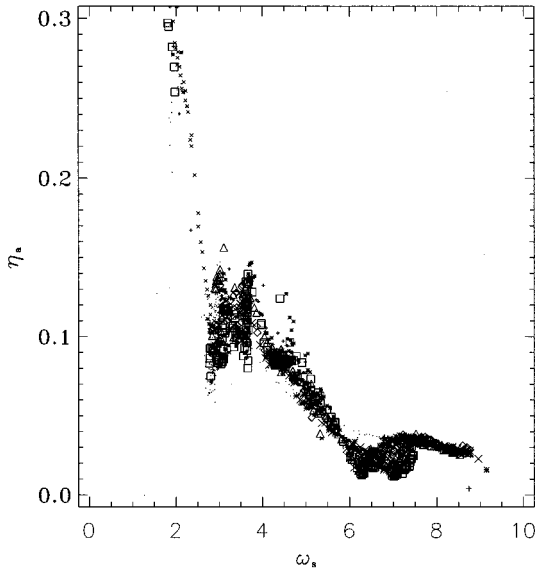


FIG. 6. Intrinsic friction  $\eta_a$  versus the frequency  $\omega_s$  of vibrations of the top substrate. The points are extracted from the  $v_s(f)$  dependences for the commensurate 300-atomic film for different values of the external friction  $\eta$ :  $\eta=0.03\omega_0$  (plus signs),  $\eta=0.04\omega_0$  (stars),  $\eta=0.05\omega_0$  (crosses),  $\eta=0.06\omega_0$  (diamonds),  $\eta=0.07\omega_0$  (triangles),  $\eta=0.08\omega_0$  (squares),  $\eta=0.09\omega_0$  (small plus signs),  $\eta=0.10\omega_0$  (small stars), and  $\eta=0.20\omega_0$  (small crosses). The data for the case of a decreasing force are shown by points.

intrinsic friction  $\eta_a$ . In the next Sec. IV we show that this explanation is valid at least qualitatively.

It is remarkable that at low velocities  $v_s$  when  $\omega_s < \Omega_{\min}$ , the intrinsic friction  $\eta_a$  is much higher than in the sliding regime. Because in this case the one-phonon mechanism of damping is not operating, the intrinsic friction has to be attributed to the highly nonlinear dynamics of the system.

For low external friction we observed also the following phenomenon: when the velocity of the top substrate reaches the very high value for which  $\omega_s > \Omega_{\max}$ , the top substrate breaks all bonds with the layer and starts to “fly.” Although this phenomena appears because we consider a top substrate made of only one atomic layer with a limited pressure  $f_{\text{load}}$  it indicates that the sharp drop of  $\eta_a$  for  $\omega_s > \Omega_{\max}$  tends to induce an unstable behavior in the system.

#### D. Variation of the mass of top substrate atoms

Finally, as Eqs. (3)–(5) also involve the masses, we made three runs for different masses of the top substrate atoms. Figure 7 shows the variation of  $\eta_a$  versus  $\omega_s$  for  $m_s=1, 3,$  and  $7$ . Although these variations are qualitatively similar to each other, quantitatively the effective friction is much lower for higher values of  $m_s$ . As will be described in the next Sec. IV, this effect can be explained as the decrease of the energy transfer when the mass of the top substrate increases and, therefore, owing to inertia the amplitude of its vertical vibrations decreases.

### IV. DYNAMICAL FRICTION FOR THE SLIDING REGIME

The results presented above show that at least in the sliding regime, i.e., for large enough velocities of the top sub-

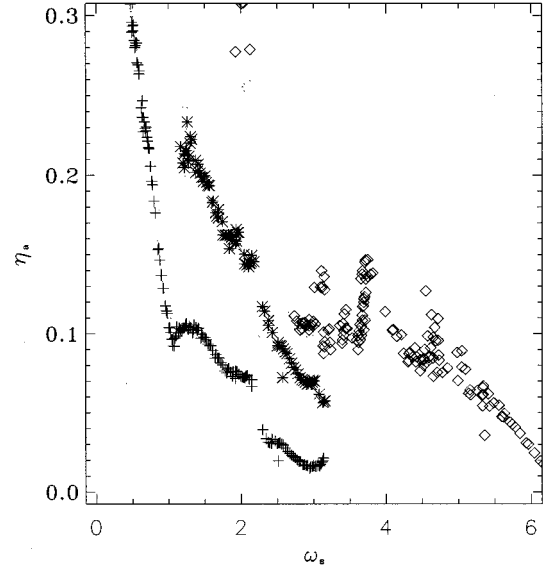


FIG. 7. The same as Fig. 6 but for different masses of the top substrate atoms:  $m_s=1$  (diamonds),  $m_s=3$  (stars), and  $m_s=7$  (plus signs). The data for the case of a decreasing force are shown by points. The external friction is  $\eta=0.1\omega_0$ .

strate, the dynamical friction may be described with simple Eqs. (3)–(5) if one can calculate the intrinsic friction coefficient  $\eta_a$ . To find  $\eta_a$ , we have to evaluate the transfer of energy to various degrees of freedom as mentioned in Sec. I. A similar calculation was performed earlier for an incommensurate adsorbed layer subjected to forces coming from one underlying substrate.<sup>6</sup> It was found that the energy transfer into phonon modes of the layer is small. The case that we consider here is different because the lubricant film is commensurate and subjected to forces coming from both substrates. When one part of the system moves with respect to another with a velocity  $v_s$ , its dynamics contains an oscillatory component with the frequency  $\omega_s = 2\pi v_s/a_s$ . Then we expect that if  $\Omega_{\min} < \omega_s < \Omega_{\max}$ , where  $\Omega_{\min}$  and  $\Omega_{\max}$ , respectively, correspond to the minimum and maximum phonon frequencies of the system, an energy transfer into phonons will occur. To estimate it, let us first calculate the vibrational spectrum of the commensurate film adsorbed on the substrate. In what follows we will ignore the loading force assuming that it is small with respect to interatomic interactions.

#### A. Phonon spectra

To calculate the spectrum, we use the Green function technique described in Refs. 8 and 11. The causal phonon Green function is defined by

$$G(t; j_1, j_2) = \sqrt{m_{j_1} m_{j_2}} \frac{1}{i\hbar} \langle T_{\text{ch}} u_{j_1}(t) u_{j_2}(0) \rangle, \quad (7)$$

where  $u_j(t)$  is the displacement of the  $j$ th atom from the equilibrium position in the Heisenberg representation,  $m_j$  is its mass, and  $T_{\text{ch}}$  is the chronological operator. The Fourier transform of  $G(t)$  satisfies the equation,

$$(\Omega^2 \mathbf{1} - \mathbf{D}) \mathbf{G}(\omega) = \mathbf{1}, \quad (8)$$

where  $\Omega^2 = \omega^2 + i\epsilon$ ,  $\epsilon > 0$ ,  $\epsilon \rightarrow 0$ . The dynamical matrix  $\mathbf{D}$  is a square matrix with the elements  $d_{j_1, j_2} = \alpha(j_1, j_2) / \sqrt{m_{j_1} m_{j_2}}$ . For a pairwise interatomic potential  $V$ , the  $\alpha(j_1, j_2)$  are defined as

$$\alpha(j_1, j_2) = \frac{\partial^2 V(x_{j_1} - x_{j_2})}{\partial u_{j_1} \partial u_{j_2}} \quad \text{if } j_1 \neq j_2 \quad (9)$$

and

$$\alpha(j, j) = \sum_{j_1 (j_1 \neq j)} \frac{\partial^2 V(x_j - x_{j_1})}{\partial u_j^2}. \quad (10)$$

The interest of the Green function technique is that additional contributions to the dynamical matrix can be introduced successively using the Dyson equation. If  $\mathbf{G}_0$  is a solution of

$$(\Omega^2 \mathbf{1} - \mathbf{D}_0) \mathbf{G}_0 = \mathbf{1}, \quad (11)$$

the solution of the Eq. (8) is given by

$$\mathbf{G} = \mathbf{G}_0 + \mathbf{G}_0 \delta \mathbf{D} \mathbf{G}, \quad (12)$$

where

$$\delta \mathbf{D} = \mathbf{D} - \mathbf{D}_0 \quad (13)$$

is the correction to the dynamical matrix. Therefore, we may start with the trivial case of a free square atomic layer, adsorb it on the substrate getting the Green function of one-layer system, and then add the second layer obtaining the Green function of a two-layer system which describes both the vibrations of the intrafilm interactions and of the substrate-film interactions.

The spatial Fourier transform over  $x$  and  $y$  of the components of the matrix function  $\mathbf{G}$  depends on  $\omega$  and a two-dimensional wave vector  $\mathbf{k} \equiv (k_x, k_y)$ . The two-particle function (7) depends also on two integers  $(n_1, n_2)$  which specify the atomic layers of the particles. Let  $n=0$  correspond to the substrate,  $n=1$  to the first film's layers, and  $n=2$  to the second layer. Besides, we have to distinguish the  $(xx)$  and  $(zz)$  components of the matrix  $\mathbf{G}$ , which correspond to the displacements in the  $x$  and  $z$  directions correspondingly. Notice that the  $(yy)$  component is equivalent to the  $(xx)$  one, and that the mixed components like  $(xz)$  are zero due to system symmetry.

The Green function of an isolated 2D square lattice is

$$G_0(1,1|xx) = [\Omega^2 - \Omega_0^2(\mathbf{k}|xx)]^{-1}, \quad G_0(1,1|zz) = 1/\Omega^2, \quad (14)$$

where

$$\Omega_0^2(\mathbf{k}|xx) = 4\omega_a^2 \sin^2\left(\frac{1}{2}a_x k_x\right). \quad (15)$$

Notice that the substrate Green function is zero, because the substrate atoms were assumed to be immobile.

Now, if we place the atomic layer on the substrate, the interaction  $V^{(a)}$  produces the following nonzero perturbation:

$$\delta D(1,1|xx) = \frac{1}{2} \delta D(1,1|zz) = \omega_0^2, \quad (16)$$

and it is easy to solve the Dyson equation (12). The Green function of the one-layer system is equal to

$$G_I(1,1|xx) = [\Omega^2 - \Omega_I^2(\mathbf{k}|xx)]^{-1},$$

$$G_I(1,1|zz) = [\Omega^2 - 2\omega_0^2]^{-1}, \quad (17)$$

where

$$\Omega_I^2(\mathbf{k}|xx) = \omega_0^2 + \Omega_0^2(\mathbf{k}|xx). \quad (18)$$

Let us now add the second-layer over the one-layer system. The interaction  $V^{(a)}$  brings the contributions

$$\delta D(1,1|xx) = \delta D(2,2|xx) = \frac{1}{2} \delta D(1,1|zz)$$

$$= \frac{1}{2} \delta D(2,2|zz) = \omega_a^2, \quad (19)$$

$$\delta D(1,2|xx) = \delta D(2,1|xx)$$

$$= \frac{1}{2} \delta D(1,2|zz) = \frac{1}{2} \delta D(2,1|zz)$$

$$= -\frac{1}{2} \omega_a^2 \left[ \cos\left(\frac{1}{2}a_x k_x\right) + \cos\left(\frac{1}{2}a_y k_y\right) \right]. \quad (20)$$

The solution of the Dyson equation gives the following Green function for the two-layer system:

$$G_{II}(2,2|xx) = \frac{\omega^2 - \omega_a^2 - \omega_0^2 - \Omega_0^2}{[\Omega^2 - \Omega_-^2(\mathbf{k}|xx)][\Omega^2 - \Omega_+^2(\mathbf{k}|xx)]}, \quad (21)$$

$$G_{II}(2,2|zz) = \frac{\omega^2 - 2\omega_a^2 - 2\omega_0^2}{[\Omega^2 - \Omega_-^2(\mathbf{k}|zz)][\Omega^2 - \Omega_+^2(\mathbf{k}|zz)]}, \quad (22)$$

where the phonon dispersion laws are

$$\Omega_{\pm}^2(\mathbf{k}|xx) = \Omega_0^2 + \omega_a^2 + \frac{1}{2} \omega_0^2 \pm \frac{1}{2} \sqrt{\omega_0^4 + 4\omega_a^4 B(\mathbf{k})}, \quad (23)$$

$$\Omega_{\pm}^2(\mathbf{k}|zz) = 2\omega_a^2 + \omega_0^2 \pm \sqrt{\omega_0^4 + 4\omega_a^4 B(\mathbf{k})}, \quad (24)$$

and

$$B(\mathbf{k}) = \frac{1}{4} \left[ \cos\left(\frac{1}{2}a_x k_x\right) + \cos\left(\frac{1}{2}a_y k_y\right) \right]^2. \quad (25)$$

The local density of "surface" phonon states is obtained from the Green function as

$$\rho_{I,II}(\omega | \dots) = -\frac{2}{\pi} \omega \int_{-\pi/a_s}^{+\pi/a_s} \frac{dk_x}{2\pi/a_s} \int_{-\pi/a_s}^{+\pi/a_s} \frac{dk_y}{2\pi/a_s}$$

$$\times \text{Im} G_{I,II}(n, n | \omega, \mathbf{k} | \dots), \quad (26)$$

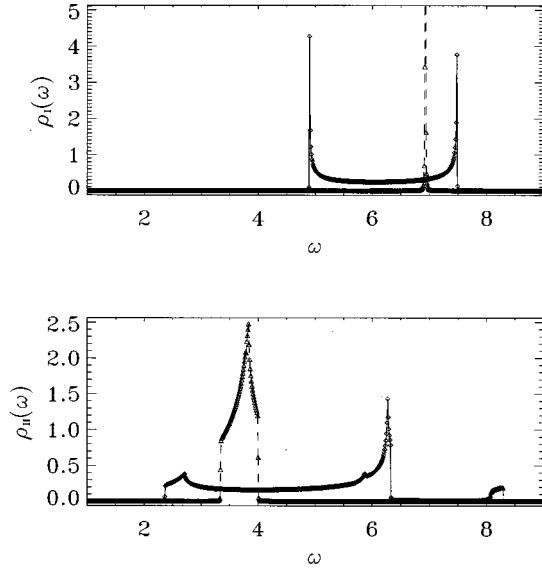


FIG. 8. Phonon spectrum of a one-layer adsorbed film  $\rho_I(\omega)$  and a two-layer film  $\rho_{II}(\omega)$ . Solid curves correspond to  $x$  vibrations, and dashed curves, to vertical vibrations.

where  $n=1$  for  $\rho_I$  and  $n=2$  for  $\rho_{II}$ . It is shown in Fig. 8

### B. Phonon mechanism of energy losses

We can now estimate the intrinsic friction  $\eta_a$ . When the top (one-layer) subsystem slides over the bottom (two-layer) subsystem, they exert on one another a periodic force

$$f_{\text{osc}}(t) \approx f_0 \cos(\omega_s t), \quad (27)$$

where the amplitude  $f_0$  is caused by subsystem's corrugation, so that  $f_0 \approx \pi \varepsilon_s / a_s$ .

According to the linear response theory,<sup>12</sup> the oscillating force (27) excites a given subsystem, increasing its energy per one time unit of the value

$$\dot{Q} = \frac{\pi f_0^2 \rho(\omega_s)}{4m_a} \quad (28)$$

(this energy is then dissipated due to external damping). Then, the intrinsic friction can be defined as

$$\eta_a = \dot{Q} / 2E_{\text{top}}, \quad (29)$$

where  $E_{\text{top}} = \frac{1}{2} m_{\text{eff}} v_s^2$  is the average kinetic energy of the top subsystem. Equation (29) may be derived if we recall that the friction force  $f = -m \eta_a v_s$  produces the work  $m \eta_a v_s^2$  per unit time.

Combining these expressions together, we come to the relationship

$$\eta_a m_{\text{eff}} \omega_s^2 \approx C \rho(\omega_s), \quad (30)$$

where the factor  $C$  is equal to  $C = \pi^5 \varepsilon_s^2 / m_a a_s^4$ , and  $\rho = \rho_I + \rho_{II}$  because there are losses both in top and bottom layers. Using the parameters  $m_a = 1$ ,  $a_s = 3$ , and the value  $\varepsilon_s \approx 1.12$  found in Sec. III, we obtain for the numerical factor the value  $C \approx 4.7$ .

To check this approximate approach, we plot in Fig. 9 the

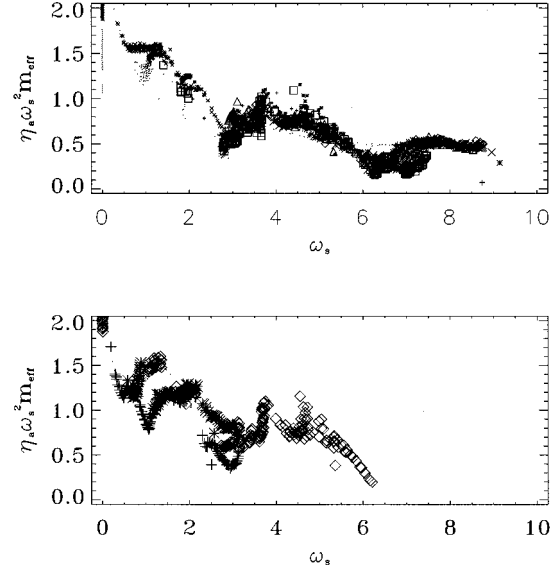


FIG. 9. Dependencies  $\eta_a \omega_s^2 m_{\text{eff}}$  versus the frequency  $\omega_s$  for different external frictions  $\eta$  (top) and different masses  $m_s$  (bottom). Notations are the same as in Figs. 6 and 7, respectively.

product  $A(\omega_s) = \eta_a m_{\text{eff}} \omega_s^2$  for the data taken from Figs. 6 and 7. Besides the low frequency contribution corresponding to the chaotic dynamics discussed in Sec. III, the simulation results show a contribution which corresponds to the frequencies where the phonon density of states is present and has peculiarities at the same frequencies as the low-frequency (long-wave) parts of the local density of phonon states of Fig. 8.

## V. CONCLUSION

In conclusion, this work shows that the dynamical friction of a thin commensurate contact must be analyzed in very different ways depending on the sliding velocity. The simpler case is the high-velocity range for which the oscillatory component of the force applied to the film, which is due to alternative bond breaking and bond forming at frequency  $\omega_s = 2\pi v_s / a_s$  is within the phonon frequencies of the layer. In this high-velocity range the lubricant film splits into two sublayers, one part attaches to the top substrate and moves together with it, while another stays with the bottom substrate. The dynamical friction can be described as the energy exchange between the top and bottom subsystems caused by excitation of phonons. The simulation results agree qualitatively with this picture, although a quantitative theory is not developed yet.

For lower velocities,  $v_s < \Omega_{\text{min}} a_s / 2\pi$ , when the one-phonon damping is forbidden and one may expect a low friction, simulations showed instead a much higher friction and a quite complicated behavior of the lubricant film, its dynamics being chaotic with intermittency properties. The results indicate that in this regime a highly nonlinear excitation and system instability play an essential role. To understand the system dynamics in the low-velocity regime, simpler models have to be studied. One can notice that the dynamics of the middle layer, moving on a pinning potential due to the layer which is below and driven by the Lennard-

Jones interactions coming from the upper layer shows a similarity with the models of blocks used to describe the dynamics of earthquakes.<sup>13,14</sup> The analogy is however not complete. Cule and Hwa<sup>14</sup> noticed that the depinning transition of the block models is characterized by a diverging correlation length, while we get a first-order transition with an anticorrelation between channels. The difference is probably due to

the disorder of the “substrate” for the block models. A modification of the block models for the low-velocity range would however deserve an investigation.

#### ACKNOWLEDGMENTS

O.M.B. acknowledges the hospitality at ENS de Lyon.

---

<sup>1</sup>B. N. J. Persson, Phys. Rev. Lett. **71**, 1212 (1993); Phys. Rev. B **48**, 18 140 (1993).

<sup>2</sup>B. N. J. Persson, J. Chem. Phys. **103**, 3849 (1995).

<sup>3</sup>M. G. Rozman, M. Urbakh, and J. Klafter, Phys. Rev. Lett. **77**, 683 (1996).

<sup>4</sup>C. Caroli and P. Nozieres, in *Physics of Sliding Friction*, edited by B. N. J. Persson and E. Tossati (Kluwer, Dordrecht, 1996).

<sup>5</sup>O. M. Braun, T. Dauxois, M. Paliy, and M. Peyrard, Phys. Rev. Lett. **78**, 1295 (1997); Phys. Rev. E **55**, 3598 (1997).

<sup>6</sup>B. N. J. Persson and A. Nitzan, Surf. Sci. **367**, 261 (1996).

<sup>7</sup>G. De Lorenzi and G. Jacucci, Surf. Sci. **164**, 526 (1985).

<sup>8</sup>A. M. Kosevich, *Fundamentals of Crystal Lattice Mechanics* (Nauka, Moscow, 1972).

<sup>9</sup>S. Aubry (private communication).

<sup>10</sup>H. G. Schuster, *Deterministic Chaos* (Physik-Verlag, Weinheim, 1984), Chap. IV.

<sup>11</sup>O. M. Braun, Surf. Sci. **213**, 336 (1989).

<sup>12</sup>L. D. Landau and E. M. Lifshitz, *Statistical Physics* (Pergamon, London, 1958).

<sup>13</sup>J. M. Carlson, J. S. Langer, and B. E. Schaw, Rev. Mod. Phys. **66**, 657 (1994).

<sup>14</sup>Dinko Cule and Terence Hwa, Phys. Rev. Lett. **77**, 278 (1996).